Hindawi
International Journal of Optics
Volume 2023, Article ID 9387645, 11 pages
https://doi.org/10.1155/2023/9387645

Research Article

Solar Light Radiometry Calibration Unit for a ScanPol Polarimeter of the Aerosol-UA Space Mission

Ivan Syniavskyi[1], **Yevgen Oberemok**[1,2], **Vassyl Danylevsky**[1,2], **Yuriy Ivanov**[1], **Roman Osypenko**[1,2], **Mikhail Sosonkin**[1], and **Gennadi Milinevsky**[1,2,3]

[1] *Main Astronomical Observatory, National Academy of Sciences of Ukraine, Kyiv, Ukraine*
[2] *Taras Shevchenko National University of Kyiv, Kyiv, Ukraine*
[3] *College of Physics, International Center of Future Science, Jilin University, Changchun, China*

Correspondence should be addressed to Ivan Syniavskyi; syniavskyi@gmail.com

Received 12 January 2023; Revised 20 May 2023; Accepted 12 June 2023; Published 10 July 2023

Academic Editor: Yuan-Fong Chou Chau

The Aerosol-UA space mission will study aerosol microphysical characteristics in the Earth's atmosphere based on the multispectral scanning polarimeter (ScanPol) and imaging polarimeter (MSIP). Both polarimeters must be precisely calibrated on the ground and in orbit to provide correct measurements. This paper considers the results of developing an experimental device for the radiometric calibration of the ScanPol. We consider the calibration unit design and operation principle to form a luminous flux with unchanged or well-predicted characteristics in a specified direction. The construction of the radiometric calibration unit is based on a sun-illuminated reflective diffuser made from the white opal glass MS20. We evaluated the scattering and polarization characteristics of the diffuser in laboratory experiments at a wide range of wavelengths. The results suggest that the polarization properties of the diffuser are negligible. The diffuser scattering parameters are close to Lambertian for illuminance conditions, which is necessary for radiometric calibration. The calibration unit was manufactured and tested during field observations of solar radiation. The results will be used for its improvement, mainly to reduce the observed stray scattered radiation entering the telescopes of the ScanPol polarization state analyzer.

1. Introduction

The primary purpose of the Aerosol-UA space mission is to determine the microphysical characteristics of aerosols in the Earth's atmosphere from the orbit using spectropolarimeters described in previous papers [1–6]. The mission is planned for launch on a subpolar sun-synchronous orbit of approximately 700 km altitude and an inclination of 98° using the YuzhSat satellite platform with a tentative launch in 2025 by the Yuzhnoye State Design Office. The MODIS and MISR instruments on the Terra satellite still operate on this orbit providing aerosol property measurements [7, 8]. Two spectropolarimeters will be installed on the following YuzhSat platform: the multispectral scanning polarimeter (ScanPol) and the multispectral imaging polarimeter (MSIP).

The ScanPol and MSIP polarimeters must be precisely calibrated on the ground and in orbit to ensure accurate measurements of solar radiation's intensity and polarization characteristics scattered by the Earth's atmosphere and surface with significant spatial coverage. To build an effective calibration procedure, polarimetric models of ScanPol and MSIP were elaborated [4]. These models take into account the main sources of measurement errors, such as shifts in the levels of dark currents, shifts in the photodetector's spectral sensitivity, and others. The possibilities and methods of polarimeter calibration are outlined in papers [4, 5]. The proposed calibration methods aim to reduce the errors in determining the degree and angle of linear polarization (DoLP and AoLP) for the ScanPol to 0.15% and 0.2°, respectively.

Various factors can affect satellite instruments' characteristics during launch and flight. Launching into orbit is characterized by strong mechanical overload and vibrations in a wide range of frequencies [9, 10]. During a space flight, when transitioning from the subsolar part of the orbit to the Earth's shadow and back, significant mechanical stresses arise in the spacecraft's structure due to sharp temperature gradients. That can cause the deformation of its units and equipment. The vacuum condition contributes to the pollution of surfaces, especially optical elements, due to the outgassing of the space platform element. Irradiation by short wavelength emission and high-energy rays and bombardment by micrometeorites also affect the characteristics of satellite instruments [11, 12]. Therefore, calibration of satellite instruments in flight is demanded to identify offset for adapt their characteristics after the spacecraft launch into orbit and throughout its functional life.

Special systems are designed for on-orbit calibration of earth-based remote sensing devices. They often use the light from the Sun and the Moon for calibration [13–18]. For example, the MODIS, VIIRS, and MISR multiangle radiometers [15, 19, 20] use the Sun's radiation for radiometric calibration. The APS polarimeter of the Glory mission, the prototype of the ScanPol, also included a unit for radiometric calibration of the instrument in orbit by the Sun,the Solar Reference Assembly [21, 22].

In the process of design a calibration device, it is necessary to consider changing conditions of illumination of the structural elements of spacecraft by the Sun. These demands are dictated by the parameters of the space platform orbit due to the apparent movement of the Sun relative to the apparatus and the configuration of the satellite depend on them, as well as by the design and parameters of the instrument itself. Finally, the Sun illumination conditions for the ScanPol polarimeter as part of the YuzhSat satellite platform are analyzed in [23].

This work aims to design and test the radiometric calibration unit based on a reflective diffuser for the multispectral scanning polarimeter ScanPol. In Section 2, the satellite platform and Aerosol-UA instruments are briefly described. The optical layout and construction of the calibration unit are discussed in Section 3, followed by the assurance scheme and test measurement results in Section 4 and 5. Finally, a short discussion and conclusions are presented in Section 6.

2. YuzhSat Satellite Platform and Complex of Scientific Equipment Aerosol-UA

The YuzhSat microsatellite platform can acquire a payload of up to 50 kg. The Aerosol-UA project will be implemented using a modification of the 30 kg platform. The payload includes the following two devices: the high precision scanning polarimeter, the ScanPol, and the wide-field multispectral imager polarimeter MSIP [2, 5], mounted in a single frame [1, 24]. The ScanPol operates in six spectral bands from the near ultraviolet to the shortwave infrared spectral with wavelengths of 370, 410, 555, 865, 1378, and 1610 nm. The ScanPol measures the three Stokes parameters I, Q, and U of the sunlight, scattered by the atmospheric aerosols and the Earth's surface, from about 200 viewing angles along a track in +50° and −60° directions from nadir [4]. The MSIP provides images of the state of the atmosphere and the Earth's surface. These images are used for the cloudiness correction of the ScanPol measurements. Using the data of both polarimeters allows for performing in-orbit calibration of the MSIP image signal by the ScanPol data. The critical element of the MSIP is the four prisms image-divided optical unit that separates a primary input image into four images on the same image sensor. The MSIP includes three polarizing paths and two radiometric paths to quantify Stokes parameters I, Q, and U in one shot in the broad field of view $60° \times 60°$ at the wavelengths 410, 555, and 865 nm and retrieve the aerosol optical depth in eight spectral wavebands. The spatial resolution of the MSIP polarimeter is 6 km on the Earth's surface at the nadir, with 15 viewing angles in a single scene [4, 5].

In Figure 1, a general view of the satellite platform with the installed payload is shown. Successful implementation of the scientific tasks of the Aerosol-UA mission is possible if the ScanPol polarimeter measures the polarimetric parameters of solar radiation scattered by the underlying aerosols and surface with an error of 0.15%.

To maintain high accuracy in measurements of polarization parameters in orbit, ScanPol is equipped with four units for in-flight calibration [4]. These units are as follows: (1) the dark unit for calibration of the polarimeter signal zero value, (2) the polarizer unit that forms a linearly polarized light with a high DoLP value and a known azimuth, (3) the depolarizer unit that forms unpolarized light, and (4) the solar radiometric calibration unit that forms light with a given intensity [23]. The first three units maintain the high polarimetric accuracy of the ScanPol. These units use as input light the solar scattered radiation by the atmosphere and Earth's surface that enters the device from the nadir.

The fourth is the ScanPol solar radiometric calibration unit, which is considered in this paper in detail. Since the Sun's radiation is well-measured, stable, and unpolarized, it is an excellent candidate to be a source of reference radiation for radiometric calibration [25]. The unit aimed to form a reference intensity of light at the entrance pupils of the ScanPol telescopes VIS1, VIS2, IR1, and IR2 using direct solar radiation. The radiometric calibration should be carried out in orbit periodically when the optimal sunlight conditions at the calibration unit's input are achieved [26].

The optical properties of the unit should not be changed noticeably during the entire operation in orbit. The spectral sunlight distortions and polarizations should not be introduced by the unit or have to be stable and well defined in the laboratory. The design of the unit has to prevent additional stray light from entering the interior of the ScanPol both during calibration and during operational measurements.

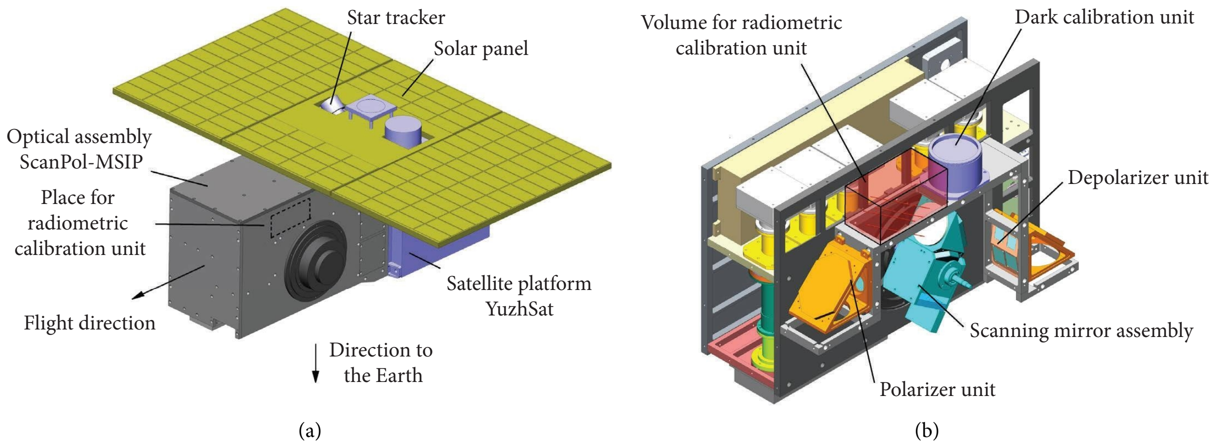

Figure 1: Aerosol-UA polarimeters onboard the YuzhSat platform: (a) general view and (b) detailed view of the front part of the ScanPol-MSIP optical assembly for installing the ScanPol radiometric calibration unit.

Due to the energy and weight limitations, it is impossible to direct solar radiation from the optical path to the calibration unit by maneuvering the device or mechanically moving any of its structural elements. The Aerosol-UA satellite will operate on a sun-synchronous orbit, which enables the positioning of the input hole of the calibration unit in an optimal way for directing solar radiation to the measurement channels once a day during the device's movement in orbit. The calibration time is reached when the satellite crosses the terminator, and the operational measurements are not performed.

The chosen optical scheme of the radiometric calibration unit allows for providing calibration procedures at the intersection with the northern part of the terminator when the calibration unit's optical axis is directed along the orbit. The deviation of the axis from this direction is determined by the parameters of the orbit and the height of the Sun above the upper edge of the atmosphere during calibration. The vertical angular size of the input diaphragm depends on the segment of orbital time (number of frames) allocated for calibration and does not exceed 2°. The horizontal angular size of the input diaphragm is determined by the distance between the positions of the Sun on the horizon during the summer and winter solstices and does not exceed 7°. In the current layout of the ScanPol-MSIP optical assembly, the space inside the assembly to install the radiometric calibration unit is limited (see Figure 1).

3. Optical Layout and Components Selection

3.1. The Optical Layout. The radiometric calibration unit operates within a 360–1700 nm spectral range and is integrated into the ScanPol-MSIP optical assembly. The optical configuration of the unit consists of a convex mirror and a diffuser (Figure 2).

Solar radiation enters the mirror that illuminates the diffuser, then the radiation scattered by the diffuser passes through the window of the scanning mirror assembly and enters the telescopes of the multispectral polarization state analyzer. The geometrical parameters of the optical system

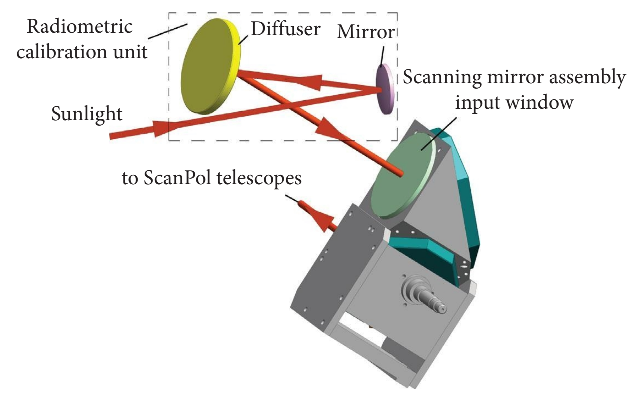

Figure 2: Optical configuration of the radiometric calibration unit.

elements are determined by the calibration unit dimensions of $90 \times 70 \times 130$ mm and by the lighting conditions of all elements' light diameters.

Another important energetical parameter of the optical system is the attenuation coefficient τ of radiation in the optical system, which is determined by the following equation:

$$\tau = \left(\frac{D_{\text{mir}}}{D_{\text{dif}}}\right)^2 \cdot r_{\text{mir}} \cdot r_{\text{dif}}, \qquad (1)$$

where D_{mir} and D_{dif} – the diameters of the mirror and diffuser, correspondingly, $r_{\text{mir}}, r_{\text{dif}}$ – the integral reflection coefficients of the mirror and diffuser. In the case of values of $D_{\text{mir}} = 32$ mm, $D_{\text{dif}} = 60$ mm, $r_{\text{mir}} = 0.7$, and $r_{\text{dif}} = 0.9$, the attenuation coefficient τ is of ~0.18.

The calibration unit creates an optical signal at the ScanPol photodetectors with values equal to or close to the signal values received from the nadir during observations of the Earth's surface. We have presented the results of developing the ScanPol multispectral polarization state analyzer in [26], where the signal-to-noise ratio was estimated for different spectral ranges based on the spectral density of the energy brightness of the Earth's surface $B(\lambda)$. It is known that the reflectivity of the Earth's surface-the Earth's albedo can vary from ~0.1 to 0.7. When observing the Earth's surface with an average albedo of 0.3, the radiation attenuation coefficient at the calibration unit should be of the same order. Therefore, the value of the attenuation coefficient $\tau = 0.18$ illustrates the agreement between signals during calibration and measurements.

3.2. The Mirror. The convex mirror forms the illumination of the diffuser by solar radiation (see Figure 2). The choice of a mirror coating is mainly determined by the operating conditions in a wide spectral range and the coating's resistance to the space environment conditions. Chromium and silver are preferable for the various mirror coatings used in the 360–1700 nm spectral range. Chromium is resistant to radiation exposure and has a reflection coefficient of 0.6–0.7 in the visible-infrared spectrum range. Silver-based mirror coating is widely used in space astronomical instruments and has a reflection coefficient of 0.85–0.95 in the spectral range of 370–900 nm. Studies show that the degradation of surface quality is insignificant [27–29].

3.3. Diffuser. Geometric parameters and material options for the radiometric calibration unit are restricted by the required angular distribution of scattered light and the diffuser spectral band. For the manufacture of diffusers (scatterers) with a wide operating optical spectrum range, which work for diffuse reflection of beams, specifically standards of whiteness, screens from magnesium oxide (MgO), barium sulfate ($BaSO_4$), and fluoropolymer are used in laboratories in different countries [30, 31]. The short-wavelength limit of reflectivity of these patterns is much less than 0.3 μm, although the slope of its decline depends on the compound of the pattern and on the way how it is applied to the surface. The long-wavelength limit is larger than 2 μm, with a decrease in reflectivity of a few percent in the spectrum area of approximately 1.5–1.6 μm.

The specified working spectral range of the ScanPol device also corresponds to some options in ceramics with diffuse reflection, for example, ceramics of the SOO-U6 type [32] or Accuflect® B6 [33]. Optical ceramics, or Irtran, are glass–type materials made from a polycrystalline array of various substances (for example, magnesium fluoride (MgF_2), magnesium oxide (MgO), and some others) by the method of hot pressing at a temperature approximately 2/3 of the melting point of the substance in a vacuum [34]. Various optical devices, including light-scattering screens, are made of these materials, mainly for the infrared part of the spectrum, which is used under high mechanical and thermal loads.

Spectralon patterns have been used for over 20 years to calibrate devices for Earth's atmosphere remote sensing and the surface from orbit [35]. These scattering screens are made of a fluoropolymer (polytetrafluoroethylene). In [36, 37] the spectral and scattering characteristics are well described. The reflectivity of Spectralon is uniform in the spectral range of 0.25–2.5 μm. The Spectralon characteristics of angular scattering are similar to those of the other scatterers. In the mentioned spectral range, when the angle of incidence varies between 50° and 60°, depending on albedo, the reflectivity of Spectralon is close to Lambertian. As with other diffusers, the Spectralon scattering indicator shows a specular component, accompanied by some degree of polarization of the scattered beams, especially for large incidence angles. Consequently, careful measurements of the angular characteristics of working samples are necessary when using such a scatterer. In space conditions, the reflectivity of spectral fluxes deteriorates due to impurities, especially in the first months, differently in different spectral channels, for example, [15, 20, 38]. However, scattering diffusers made of Spectralon are used as a convenient working tool for orbital calibration for remote sensing satellite instruments, such as MODIS and VIIRS [15], MISR [39], POSP [40], OMI [41], and others. Spectralon was used in the APS instrument of the Glory satellite [13, 22]. Various auxiliary devices are used to assess and consider the degradation of such scatterers, as mentioned in [18, 20, 41], and special spacecraft maneuvers are aimed at the Moon [18, 20, 22].

Reflectors made of white opal glass are used mainly as whiteness standards in the visible part of the spectrum (0.4–0.75 μm), where their spectral properties are well studied (see, for example, [42–44]. However, as it is shown in the cited publications, white opal glass samples of the types MS20 and OHC1–OHC4 which are, in particular, fabricated in Ukraine (https://ipz.com.ua/), as well as white opal glass samples of the types 2015 and 2016 manufactured in the USA, have high reflectance at both limits of the indicated visual part of the spectrum. In [32], the spectral properties of the diffuse reflection of a sample of white opal glass MS20 in the range of 0.3–2.4 μm is given. At wavelengths of 350 nm and 2000 nm, the reflection coefficient of this MS20 is approximately 0.80. The angular properties of the MS20 diffuse reflection were also studied in detail by various authors and are given in many publications, particularly in [32, 33, 42–44].

Despite the relatively low reflectance of this sample compared to the Spectralon, the MS20's other scattering characteristics are comparable. Therefore, given its availability in Ukraine, MS20 is considered promising for use as a diffuser screen in the ScanPol polarimeter radiometric calibration unit of the Aerosol-UA space mission.

4. Estimation of the Diffuser's Scattering Properties

In the radiometric calibration unit, we use the reflective white opal glass MS20 (AlF_3-SiO_2) based diffuser with a diameter of 60 mm. We estimate its scattering properties in a series of experiments. First, the Mueller polarimeter with a wavelength of 632.8 nm was used to estimate the polarization effect and complete Mueller polarimetry. Note that the operation features of ScanPol allow polarization measurements and polarization calibration regardless of radiometric calibration [4]. The partial polarization in the radiation scattered by the diffuser will redistribute the intensities in the ScanPol channels with orthogonal polarizations but will not change the total intensity. This circumstance makes it possible not to consider the partial polarization of the radiation scattered by the diffuser.

The experiment's geometry is shown in Figure 3, where PSG–polarization state generator and PSA-polarization state analyzer, Θ_i-the angle of light incidence, and Θ_s-scattering angle. The PSG includes a beam expander that broadens the input laser beam to a 10 mm in diameter. The measurements were carried out on the incident plain. The design features of the measuring setup determine the minimum possible angle between the direction of the incident beam and the direction of observation as $\Theta_i + \Theta_s = 10^\circ$. The diffuser is mounted at the rotating stage to change the incident angle. The range of observable scattering angles is expanded with increasing incidence angle.

The angular dependences of Mueller matrix elements were measured for the cases when the light incident the diffuser at angles of $\Theta_i = 0^\circ$, 15°, and 30°. A measurement error of normalized Mueller matrix elements δm_{ij} was 1.5%. The results demonstrated that the values of only the normalized Mueller matrix diagonal elements were far from zero. The absolute values of these elements slightly decrease when the scattering angle grows. Other matrix elements are close to zero within the error range, except for m_{12}. The dependencies of the mentioned nonzero Mueller matrix elements are shown in Figure 4. Therefore, the diffuser does not produce any instrumental polarization under the given conditions since the DoLP for totally depolarized input is determined by the following equation:

$$\mathrm{DoLP} = \sqrt{m_{21}{}^2 + m_{31}{}^2}. \tag{2}$$

Depolarizing effect of the diffuser for linear polarized input light at wavelength 632.8 nm can be expressed by the following equation:

$$\mathrm{DoLP} \le \sqrt{m_{22}{}^2 + m_{33}{}^2} \approx 0.14, \tag{3}$$

since the Mueller matrix of the diffuser is diagonal and the maximum number of diagonal elements' modules is about 0.14. In (3), an equal sign should be used for totally polarized linear input light. The diffuser's depolarization effect grows when the scattering angle increases, as shown in Figure 4.

Second, the bidirectional reflection distribution function (BRDF) values were obtained for the MS20 sample when the laser sources with wavelengths 450 nm, 532 nm, 632.8 nm, and 1064 nm were used for the geometry shown in Figure 3 with modification. The reference intensity channel was introduced to compensate for the sources' signal flux, and the PSG and PSA were removed. The results are presented for normalized BRDF in Figure 5. The BRDF is normalized on a value corresponding to the measured one at $\Theta_s = 10^\circ$ since it is a minimal observable scattering angle at normal light incidence ($\Theta_i = 0^\circ$).

The irregularities on dependencies in Figure 5 could be explained by an error in the angular positioning of the receiving part Figure 3 which was of $\delta\Theta_s \approx 1^\circ$. There is also some bias in the axis of the rotating stage from the axis of measurement arm rotation at which the receiving part is mounted. The BRDF of Lambertian scattering is a strain line parallel to X-axis. In Figure 5, the scattering of the diffuser is the closest to the Lambertian scattering the closer the incidence angle to 45°. In general, the scattering of the studied diffuser deviates from the Lambertian scattering by less than 1% within the 20° range of scattering angle for all incidence angles at all used spectral wavelengths.

5. Test Measurements with the Radiometric Calibration Unit

The experimental design of the calibration unit is presented in Figure 6. A unit of diaphragms is attached to the Aerosol-UA assembly where the convex mirror and the diffuser are fixed, forming the working FOV of the calibration unit, which is of 7° in the horizontal plane and 2° in the vertical plane [23]. Additional intermediate diaphragms are also placed in the diaphragm unit to minimize stray light.

In the standard the ScanPol-MSIP optical assembly for the test experiment of the calibration unit, a scanning mirror unit, and a camera with a matrix detector for recording the light flux was installed (Figure 7(a), upper panel). The upper part of Figure 7 schematically shows the operation of the input lenses of the ScanPol multispectral polarization state analyzer. Sunlight illuminates the diffuser of the calibration unit. The scattered radiation passes through the mirror scanning unit and enters the input lenses of telescopes VIS1, VIS2, IR1, and IR2, which focus the light beams in their focal planes, where the field diaphragms are installed. Next, the light passes through collimators, Wollaston prisms, dichroic mirrors, spectral filters, and camera lenses and is focused on sensors. This part is described in detail in our paper [26].

However, we performed the calibration unit performance test at the first step without using the multispectral polarization state analyzer to evaluate the light beams formed after the field apertures by the scheme in Figure 7(a) in the lower panel. In this case, the Hartmann diaphragm replaces the input lenses (telescopes) with apertures equal to their light diameters. Finally, a focusing lens with the matrix detector is installed behind the diaphragm.

The Hartmann diaphragm can be installed in position 1 or 2. Position 2 is preferable because it is more convenient and the diaphragm will not glare in the sunlight. The aperture of T in the focal plane of the lens is essential. It ensures the telecentric path of the beams, and the Hartmann diaphragm separates the working areas of the diffuser. If the detector is defocused so that the camera lens builds an image of the scatterer, we will get a matching of all scheme elements. Therefore, we model the operation of the input lenses of the ScanPol multispectral polarization state analyzer and evaluate the light fluxes after the field diaphragms. The focusing lens with the matrix detector was also placed in the standard assembly of the ScanPol-MSIP unit and installed on the roof of the laboratory building. Finally, the entrance hole of the external diaphragm was directed to the Sun, with the subsequent recording of the solar radiation fluxes (Figure 7(b)).

To evaluate the work efficiency of the calibration unit in dependence on the change in the angle of the position of the

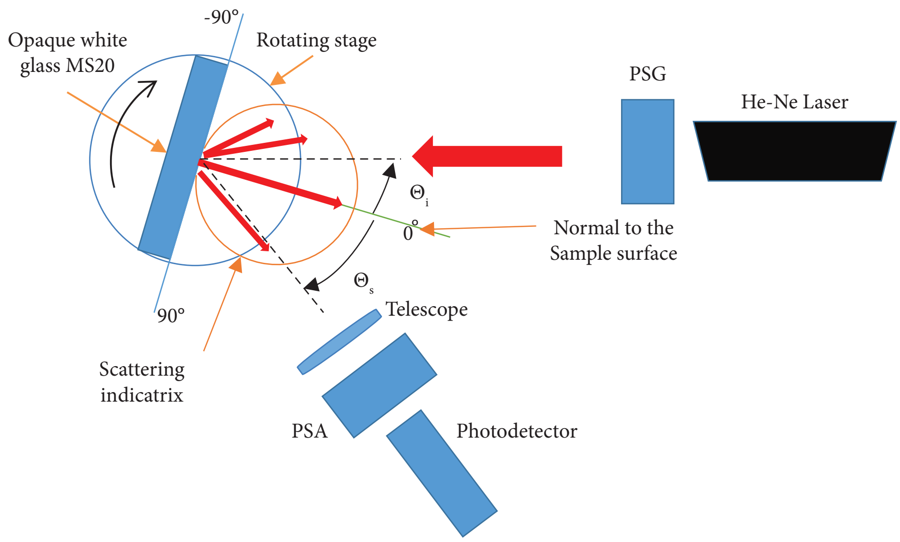

Figure 3: Geometry of polarimetric experiments with white opal glass MS20.

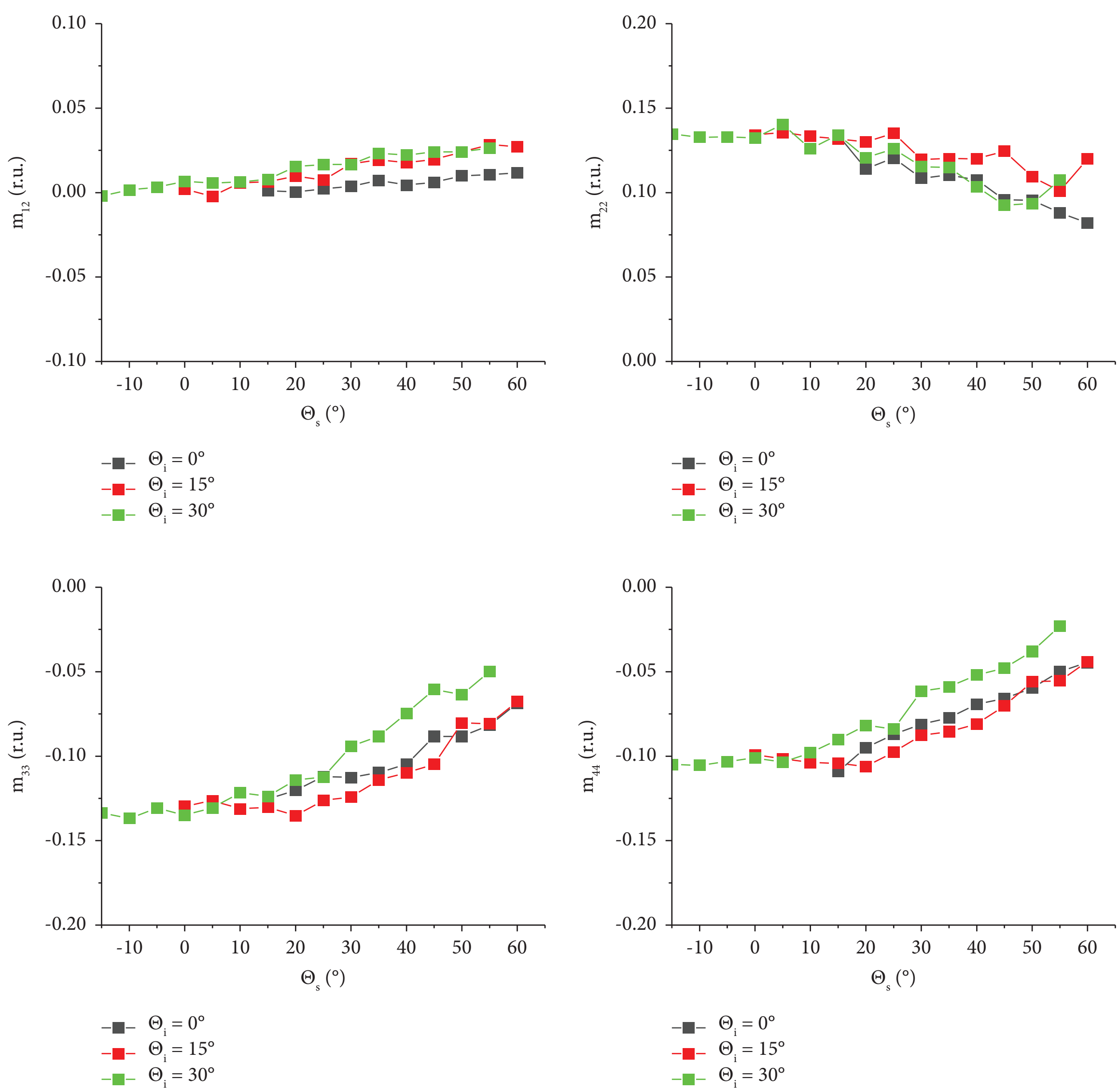

Figure 4: Dependencies of normalized by m_{11} nonzero Mueller matrix elements for the white opal glass MS20 (in relative units) at scattering angles for incidence angles $\Theta_i = 0^\circ$, 15°, and 30° of light wavelength 632.8 nm.

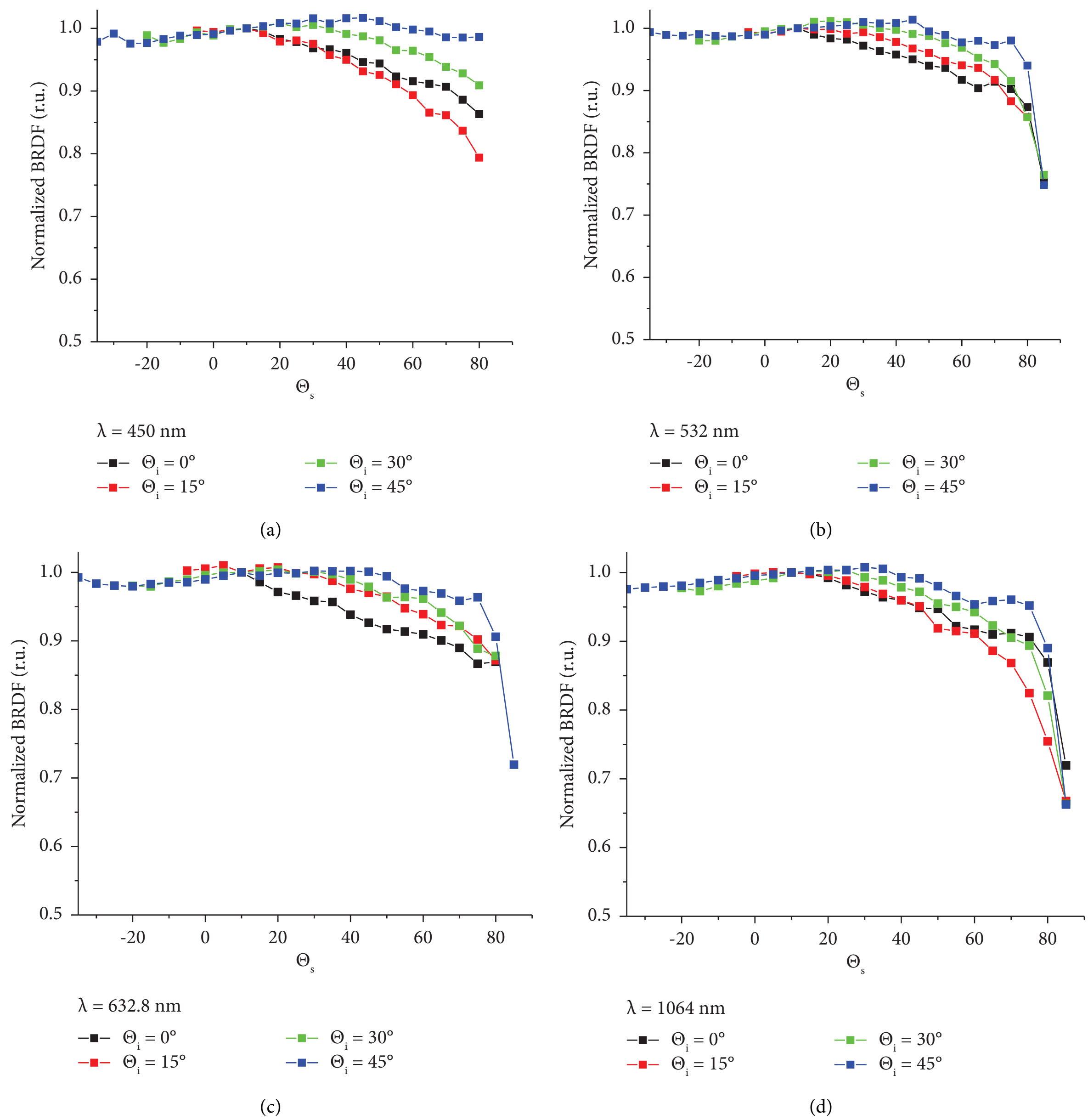

FIGURE 5: Dependencies of normalized BRDF (in relative units) for sample diffuser MS20 on scattering angle for light incidence $\Theta_i = 0^\circ$, 15°, 30°, 45° at wavelengths (a) 450 nm, (b) 532 nm, (c) 632.8 nm, and (d) 1064 nm.

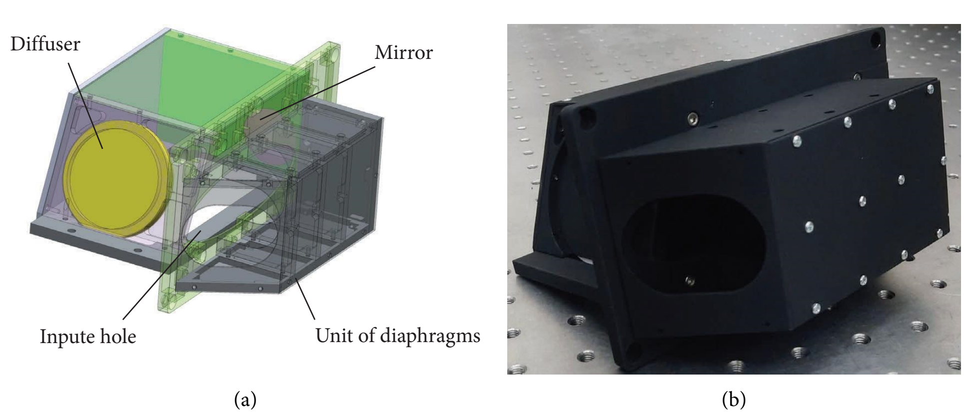

FIGURE 6: General design of the radiometric calibration unit: (a) computer model of the unit and (b) view of the manufactured calibration unit.

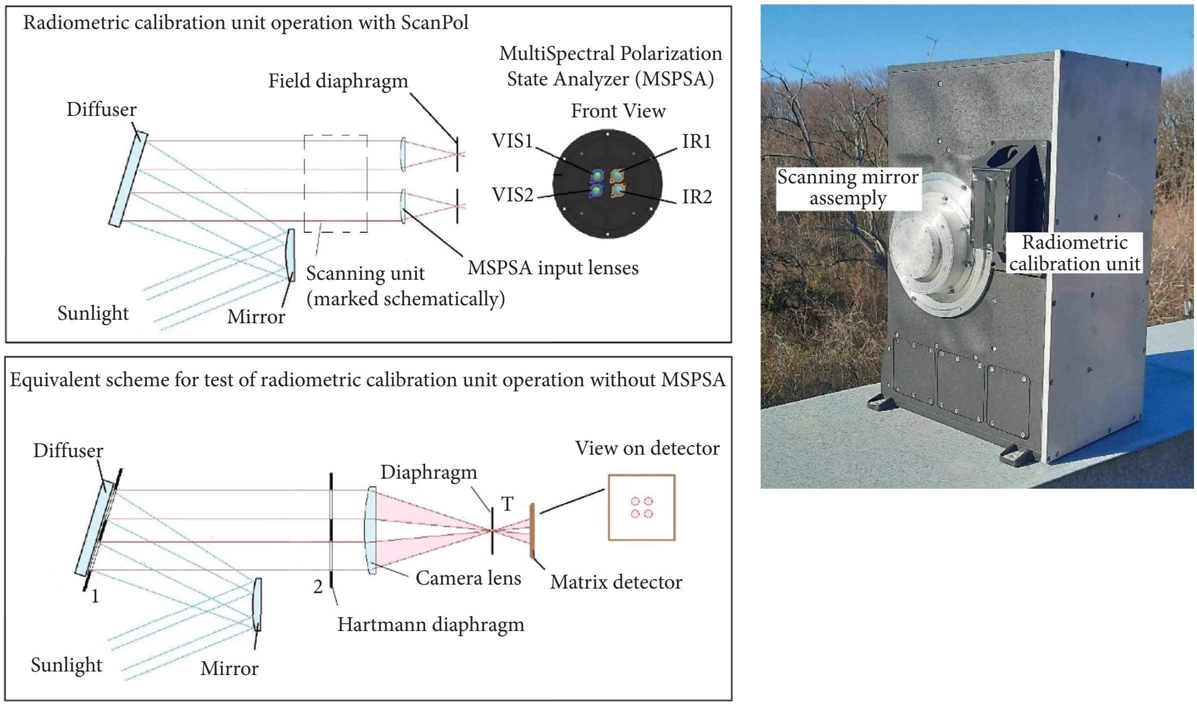

(a) (b)

Figure 7: (a) The test field measurements equivalent scheme (lower panel) to evaluate the operation of the calibration unit, the scheme of the calibration unit's operation with the multispectral polarization state analyzer telescopes (VIS1, VIS2, IR1, and IR2) is shown in upper panel and (b) the solar radiometric calibration unit with the ScanPol-MSIP optical assembly during field measurements.

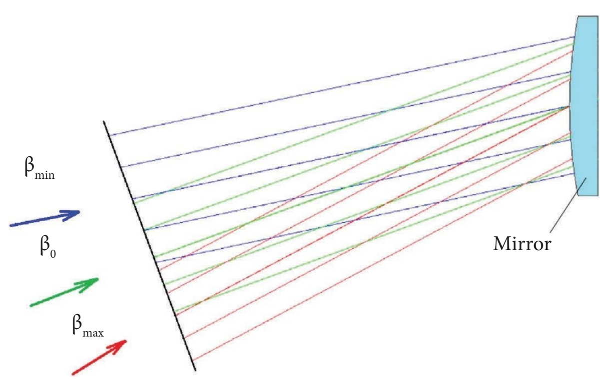

Figure 8: Schematic representation of the changes in the angle of 7° of the Sun positions between $\beta_{\min}$ and $\beta_{\max}$ during calibration.

Table 1: Digital numbers W proportional to light intensity for different angles β of the Sun's positions.

ScanPol telescopes	$W\ (\beta_0)$	$W\ (\beta_{\min})$	$W\ (\beta_{\max})$	The difference in the intensity relative to the center of the FOV	
				$\Delta\ W\ (\beta_{\min})$, %	$\Delta\ W\ (\beta_{\max})$, %
VIS1	20345	20321	20176	0.16	0.83
VIS2	15738	15786	15715	0.3	0.14
IR1	28621	27307	27252	4.5	4.8
IR2	23218	22216	22016	4.3	5.2

Sun, the FOV was scanned along the central axis of the external aperture (Figure 8).

Quantitative characteristics of the radiometric calibration unit recorded by the detector (Figure 7(a)) depending on the Sun angle position are presented in digital numbers W proportional to averaged light intensity shown in Table 1.

In Table 1, the W values are presented, which are proportional to light intensity at an enter in four ScanPol telescopes VIS1, VIS2, IR1, and IR2 for different angles β of the Sun's positions. The measurement scheme is shown in Figure 7(a) (lower panel). During calibration, the sunlight enters the FOV calibration unit, illuminates the diffuser ($\beta_{\min}$), and is passes through the center of the FOV (β_0), next to the edge of the FOV ($\beta_{\max}$). A matrix detector measures the signal value W in each of the described positions.

6. Discussion and Conclusions

The design features of the YuzhSat platform and the limited volume allocated to the satellite's payload made it possible to design a calibration unit based only on a reflective diffuser that determines the illumination of the diffuser in a range of incidence angles of $14.5^{\circ} \div 21.5^{\circ}$. The angle values depend on the change of season. At the same time, the scattered light from the diffuser comes to the input window of the scan unit from a direction near the scattering angle in the range of $-1^{\circ} \div 1^{\circ}$. The input window looks directly at the diffuser. These angles come up so that we scan the diffuser and get multiple signal readings.

As mentioned above, the scattering properties of the considered diffuser are close to the Lambertian scattering within mentioned incidence and scattering angles, at least for the spectral range of 450–1064 nm. Therefore, providing the size of light spots on the diffuser are larger than the FOV of telescopes, it will be possible to significantly reduce intensity fluctuations in the measuring channels when the Sun is displaced relative to the input window of the calibration node during radiometric calibration.

The core part of the radiometric ScanPol calibration is to obtain a calibration coefficient A_r in the calibration model of the polarimeter that was described in detail in [4]. We demonstrate (see Figure 4) that the diffuser based on the white opal glass MS20 at wavelength 632.8 nm does not produce stray instrumental polarization under considered conditions when the diameter of the illuminated diffuser's area is at least 10 mm. At the same time the stray instrumental polarization of the convex mirror can be significant for off-normal light incidence cases. The theoretical analysis, involving Fresnel equations, carried out for silver and chromium mirrors, shows the DoLP of the reflected sunlight that incidents the mirrors at the angle 17° doesn't exceed 0.6% for silver mirrors and does not exceed 5% for chromium mirrors for the ScanPol spectral range of 360–1700 nm. However, the diffuser will significantly reduce the DoLP. For instance, for wavelength 632.8 nm, the diffuser reduces DoLP for approximately seven times. Therefore, the effect of the instrumental polarization of the convex mirror is also negligible for the considered calibration unit design. In addition, as mentioned in Section 4, even a significant partial polarization of radiation scattered by a diffuser (for example, at other wavelengths) will only redistribute the intensities in ScanPol channels with orthogonal polarizations. But it will not change the total intensity I, which should be used to calculate the radiometric coefficient A_r. In this case, the following expression should be used:

$$A_r = \frac{2I\left(1 + q_{\mathrm{inst}}q + u_{\mathrm{inst}}u\right)}{\left(\mathrm{RD}_0 + K1 \cdot \mathrm{RD}_{90}\right)} \approx \frac{2I}{\left(\mathrm{RD}_0 + K1 \cdot \mathrm{RD}_{90}\right)}, \quad (4)$$

where RD_0 and RD_{90} is the zero-signal bias compensated digital values from the output of the ScanPol channels with analyzers azimuths $\alpha = 0^{\circ}$ and 90° correspondingly; q and u-second and third Stokes parameters of solar radiation scattered by diffuser; q_{inst} and u_{inst} – second, and third Stokes parameters of stray instrumental polarization introduced by the scan system of ScanPol; $K1$ – isotropic gain coefficient for 90° ScanPol channel [4]. The values q_{inst}, u_{inst} and $K1$ are calibrated regardless of A_r. In equation (4), $|q_{\mathrm{inst}}\, q + u_{\mathrm{inst}}u| \leq 10^{-4}$ for DoLP of radiation scattered by diffusor is up to 2%. The problem of the possible diffuser's characteristics degradation due to contamination can be reduced by the preliminary cleaning procedure.

The parasitic scattering inside the radiometric calibration unit will introduce errors into the calibration, which must be minimized, for example, by including diaphragms. Computer modeling of additional apertures and blends, their sizes, shapes, and positions, which can significantly reduce scattered parasitic radiation in the calibration unit, was also previously explored.

Finally, our estimation of the diffuser's characteristics is qualitative. Nevertheless, it gives us reason to assume that the calibration unit will precisely provide on-orbit radiometric calibration for ScanPol. During the unit's operation test, the measurements of light beams from the Sun were carried out according to the ScanPol scheme of operation. We obtained the relative intensity of the light beams entering the input of the multispectral polarization state analyzer for four channels at different positions of the Sun. We also scanned the entire FOV of the calibration unit. The maximum irregularity of the light beam intensity from one edge of the FOV to the other is less than 1% for VIS channels and less than 5% for IR channels. Such a sufficiently large range of irregularity is primarily associated with the scattered parasitic radiation entering the input of the optical channels of the Stokes parameter converter and requires further, more detailed research.

These results are necessary for specifying ways to improve the parameters of the radiometric calibration unit and for a more detailed analysis of the real parameters of the scanning unit. At the next stage, we plan to analyze the light beams in the working spectral channels of ScanPol in the range of 360–1700 nm using a multispectral polarization state analyzer and measure the light beams with real photodetectors.

Data Availability

The data used to support the findings of this study are available from the corresponding author upon request.

Conflicts of Interest

The authors declare that they have no conflicts of interests regarding the publication of this paper.

Acknowledgments

The research was supported by the National Academy of Sciences of Ukraine within the Target Complex Program of Scientific Space Explorations for 2018–2022, Taras Shevchenko National University of Kyiv, under agreement BF/30-2021, and the International Center of Future Science (College of Physics, Jilin University, Changchun, China). This study was also supported in part by the Program of Studies and Innovations of the European Union "Horizon 2020" under grant agreement Marie Sklodowska no. 778349 GRASP-ACE and the Innovation Program under grant agreement ACTRIS-2 no. 654109.

References

[1] I. I. Syniavskyi, G. P. Milinevsky, Y. S. Ivanov et al., "Methodology, hardware implementation, and validation of satellite remote sensing of atmospheric aerosols: first results of the Aerosol-UA space experiment development," *Kosmična nauka ì tehnologìâ*, vol. 21, no. 3, pp. 9–17, 2015.

[2] G. Milinevsky, Y. Yatskiv, O. Degtyaryov et al., "New satellite project Aerosol-UA: Remote sensing of aerosols in the terrestrial atmosphere," *Acta Astronautica*, vol. 123, pp. 292–300, 2016.

[3] O. Dubovik, Z. Li, M. I. Mishchenko et al., "Polarimetric remote sensing of atmospheric aerosols: instruments, methodologies, results, and perspectives," *Journal of Quantitative Spectroscopy and Radiative Transfer*, vol. 224, pp. 474–511, 2019.

[4] G. Milinevsky, Y. Oberemok, I. Syniavskyi et al., "Calibration model of polarimeters on board the Aerosol-UA space mission," *Journal of Quantitative Spectroscopy and Radiative Transfer*, vol. 229, pp. 92–105, 2019.

[5] I. Syniavskyi, Y. Oberemok, V. Danylevsky et al., "Aerosol-UA satellite mission for the polarimetric study of aerosols in the atmosphere," *Journal of Quantitative Spectroscopy and Radiative Transfer*, vol. 267, Article ID 107601, 2021.

[6] I. Syniavskyi, Y. Oberemok, Y. Ivanov, M. Sosonkin, V. Kireyev, and K. Akinin, "Scan mirror assembly for the multispectral scanning polarimeter of aerosol-UA space mission," *International Journal of Optics*, vol. 2021, Article ID 8854505, 12 pages, 2021.

[7] D. Tanré, Y. J. Kaufman, M. Herman, and S. Mattoo, "Remote sensing of aerosol properties over oceans using the MODIS/EOS spectral radiances," *Journal of Geophysical Research: Atmospheres*, vol. 102, no. 14, pp. 16971–16988, 1997.

[8] B. Gérard, J.-L. Deuzé, M. Herman et al., "Comparisons between POLDER 2 and MODIS/Terra aerosol retrievals over ocean," *Journal of Geophysical Research*, vol. 110, no. 24, Article ID D24211, 2005.

[9] T. D. Scharton, "Vibration and acoustic testing of spacecraft," *Sound and Vibration*, vol. 36, no. 6, pp. 14–18, 2002.

[10] J. P. Arenas and R. N. Margasahayam, "Noise and vibration of spacecraft structures," *Ingeniare: Revista Chilena de Ingeniería*, vol. 14, no. 3, pp. 251–264, 2006.

[11] C. Soares and R. Mikatarian, "Understanding and control of external contamination on the international space station," in *Proceedings of the 9th International Symposium on Materials in a Space Environment*, pp. 189–195, Noordwijk, The Netherlands, September 2003.

[12] S. Bäumer and H. Werij, "Space optics," *Advances in Optical Technologies*, vol. 7, no. 6, pp. 351-352, 2018.

[13] B. Cairns and I. Geogdzhayev, "Aerosol polarimetry sensor calibration," GSFC, Greenbelt, MD, USA, Document GSFC 421.7-70-03, 2010.

[14] R. E. Eplee, G. Meister, F. S. Patt et al., "On-orbit calibration of SeaWiFS," *Applied Optics*, vol. 51, no. 36, pp. 8702–8730, 2012.

[15] X. Xiong and J. J. Butler, "MODIS and VIIRS calibration history and future outlook," *Remote Sensing*, vol. 12, no. 16, pp. 2523–2531, 2020.

[16] X. Xiong, J. Sun, S. Xiong, and W. L. Barnes, "Using the Moon for MODIS on-orbit spatial characterization," *SPIE Proceedings*, vol. 5234, pp. 480–487, 2004.

[17] Z. Wang, X. Xiong, J. Fulbright, and N. Lei, "VIIRS day/night band radiometric calibration stability monitoring using the Moon," *Journal of Geophysical Research: Atmospheres*, vol. 122, no. 11, pp. 5616–5624, 2017.

[18] W. Wang, L.-M. Zhang, W. Xu, X.-L. Si, and W.-X. Huang, "A method for monitoring solar diffuser's bidirectional reflectance distribution function degradation in geostationary orbit," *European Journal of Remote Sensing*, vol. 53, no. 1, pp. 132–144, 2020.

[19] M. Dinguirard and P. N. Slater, "Calibration of space-multispectral imaging sensors: A review," *Remote Sensing of Environment*, vol. 68, no. 3, pp. 194–205, 1999.

[20] X. Xiong, J. Sun, W. Barnes et al., "Multiyear on-orbit calibration and performance of Terra MODIS reflective solar bands," *IEEE Transactions on Geoscience and Remote Sensing*, vol. 45, no. 4, pp. 879–889, 2007.

[21] R. J. Peralta, C. Nardell, B. Cairns et al., "Aerosol polarimetry sensor for the glory mission," *SPIE Proceedings*, vol. 6786, Article ID 67865, 2007.

[22] S. Persh, Y. J. Shaham, O. Benami et al., "Ground performance measurements of the glory aerosol polarimetry sensor," *Earth Observing Systems*, vol. 7807, pp. 780703–780711, 2010.

[23] I. I. Syniavskyi, V. O. Danylevsky, Y. A. Oberemok et al., "Radiometric on-orbit calibration of the aerosol-UA mission scanning polarimeter: technique, design elements, and illumination angles," *Kinematics and Physics of Celestial Bodies*, vol. 39, no. 1, pp. 49–69, 2023.

[24] I. Syniavskyi, Y. S. Ivanov, M. Sosonkin, G. P. Milinevsky, and G. V. Koshman, "Multispectral imager polarimeter of the AEROSOL-UA space project," *Kosmìčna nauka ì tehnologìâ*, vol. 24, no. 3, pp. 23–32, 2018.

[25] J. C. Kemp, G. D. Henson, C. T. Steiner, and E. R. Powell, "The optical polarization of the Sun measured at a sensitivity of parts in ten million," *Nature*, vol. 326, no. 6110, pp. 270–273, 1987.

[26] I. Syniavskyi, Y. Oberemok, Y. Ivanov, and M. Sosonkin, "Multispectral polarization state analyzer of scanning polarimeter ScanPol," *International Journal of Optics*, vol. 2020, Article ID 1695658, 15 pages, 2020.

[27] R. A. Keski-Kuha, C. W. Bowers, M. A. Quijada et al., "James Webb Space Telescope optical telescope element mirror coatings," *Space Telescopes and Instrumentation 2012: Optical, Infrared, and Millimeter Wave*, vol. 8442, 2012.

[28] D. Garoli, L. V. Rodriguez De Marcos, J. Larruquert, A. Corso, R. Proietti Zaccaria, and M. Pelizzo, "Mirrors for space telescopes: degradation issues," *Applied Sciences*, vol. 10, no. 21, p. 7538, 2020.

[29] S. Baccaro, A. Piegari, I. Di Sarcina, and A. Cecilia, "Effect of/spl gamma/irradiation on optical components," *IEEE Transactions on Nuclear Science*, vol. 52, no. 5, pp. 1779–1784, 2005.

[30] A. Höpe, "Diffuse reflectance and transmittance," *Experimental Methods in the Physical Sciences*, vol. 46, pp. 179–219, 2014.

[31] Shimadzu, "Example of reflectance measurement using integrating sphere: difference of spectra depending on white reference plate," *Shimadzu Excellence in Science Application News*, Shimadzu Corporation, Kyoto, Japan, 2021.

[32] O. S. Dymshits, A. A. Zhilin, A. V. Shashkin, V. A. Parfinskiĭ, and A. Y. Polushkin, "The new SOO-U6 and SOO-I8 light-scattering glass-ceramics," *Journal of Optical Technology*, vol. 76, no. 3, pp. 158-159, 2009.

[33] Accuratus Corporation, "Reflectance characteristics of Accuflect™ light reflecting ceramic," 2010, http://accuratus.com.

[34] W. L. Wolf and G. J. Zissis, *The Infrared Handbook*, SPIE, Washington DC, USA, 1978.

[35] J. Sun and X. Xiong, "Solar and lunar observation planning for Earth-observing sensor," *SPIE Proceedings*, vol. 8176, pp. 817610-817611, 2011.

[36] G. T. Georgiev and J. J. Butler, "BRDF study of gray-scale Spectralon," *SPIE Proceedings*, vol. 7081, pp. 708107–708111, 2008.

[37] C. J. Bruegge, A. E. Stiegman, R. A. Rainen, and A. W. Springsteen, "Use of Spectralon as a diffuse reflectance standard for in-flight calibration of earth-orbiting sensors," *Optical Engineering*, vol. 32, no. 4, pp. 805–814, 1993.

[38] A. E. Stiegman, C. J. Bruegge, and A. W. Springsteen, "Ultraviolet stability and contamination analysis of Spectralon diffuse reflectance material," *Optical Engineering*, vol. 32, no. 4, pp. 799–804, 1993.

[39] N. L. Chrien, C. J. Bruegge, and R. R. Ando, "Multi-angle imaging SpectroRadiometer (MISR) on-board calibrator (OBC) in-flight performance Studies," *IEEE Transactions on Geoscience and Remote Sensing*, vol. 40, no. 7, pp. 1493–1499, 2002.

[40] Y. Hongchun, Y. Benyong, S. Maoxin, Z. Peng, S. Xiaobing, and H. Jin, "Onboard polarimetric calibration methods of spaceborne scanning polarimeter," *Chinese Journal of Lasers*, vol. 45, no. 11, Article ID 1110002, 2018.

[41] M. R. Dobber, R. J. Dirksen, P. F. Levelt et al., "Ozone monitoring instrument calibration," *IEEE Transactions on Geoscience and Remote Sensing*, vol. 44, no. 5, pp. 1209–1238, 2006.

[42] V. R. Weidner, *White Opal Glass Diffuse Spectral Reflectance Standards for the Visible Spectrum (SRM'S 2015 and 2016)*, National Bureau of Standards Special Publication, Washington, DC, USA, 1983.

[43] F. J. J. Clarke, F. A. Garforth, and D. J. Parry, "Goniophotometric and polarization properties of white reflection standard materials," *Lighting Research and Technology*, vol. 15, no. 3, pp. 133–149, 1983.

[44] A. Höpe and K.-O. Hauer, "Three-dimensional appearance characterization of diffuse standard reflection materials," *Metrologia*, vol. 47, no. 3, pp. 295–304, 2010.